Facial Transplantation: An Anatomic and Surgical Analysis of the Periorbital Functional Unit

Dalibor Vasilic, M.D.
John H. Barker, M.D., Ph.D.
Ross Blagg, M.S.
Iain Whitaker, M.D.
Moshe Kon, M.D., Ph.D.
M. Douglas Gossman, M.D.

Louisville, Ky.; and Utrecht, The Netherlands

Background: Complete loss of eyelid pair is associated with chronic discomfort, corneal ulceration, and visual impairment. Contemporary reconstructive techniques rarely provide functionally acceptable results. Composite tissue allotransplantation may provide a viable alternative. This study reports on neurovascular anatomy and technical details of harvesting an isolated periorbital unit and discusses its functional potential.
Methods: Twenty-four hemifaces (12 fresh cadavers) were dissected to study surgically relevant neurovascular structures and to develop an efficient harvest method. Angiographic analysis was performed in seven hemifaces following harvest.
Results: The superficial temporal and facial vessels demonstrated consistent location and diameters. Anatomic variability was characterized by the absence of the frontal branch of the superficial temporal artery or facial-to-angular artery continuation, but never of both vessels in the same hemiface. Angiographic analysis demonstrated filling of the eyelid arcades, provided the anastomoses between the internal and external carotid branches were preserved. The facial nerve exhibited consistent planar arrangement and diameters in the intraparotid and proximal extraparotid regions, but less so in the distal nerve course. The inferior zygomatic and buccal branches frequently coinnervated the orbicularis oculi and lower facial muscles with an unpredictable intermuscular course. Based on the foregoing, an effective surgical harvest of the periorbital composite was developed.
Conclusions: Surgical harvest of a functional periorbital allotransplant is technically feasible. Revascularization of the isolated periorbital unit is influenced by variations in regional anatomy and cannot be guaranteed by a single vascular pedicle. The orbicularis oculi muscle and its innervation can be preserved, and recovery, albeit without the certainty of reflexive blinking, is expected. (*Plast. Reconstr. Surg.* 125: 125, 2010.)

Loss of an ipsilateral or bilateral eyelid pair is associated with chronic discomfort, corneal ulceration, and visual loss. Current reconstructive methods include retrieval and reattachment of original tissues[1–3] or replacement with autologus grafts and flaps from remote sites.[4,5] Given the complex functional anatomy of the eyelid unit, this injury presents a reconstructive challenge that is typically associated with poor functional and aesthetic outcomes (Fig. 1). Revision surgery provides limited improvement and carries the burden of additional donor-site morbidity.

Composite tissue allotransplantation, introduced recently for facial reconstruction, could provide an alternative to current treatments. The cases performed so far have transplanted nasal

From the Department of Surgery and the Division of Plastic and Reconstructive Surgery, University of Louisville, and the Department of Plastic, Reconstructive, and Hand Surgery, University of Utrecht.
Received for publication March 16, 2009; accepted July 10, 2009.
Presented at the European Association of Plastic Surgeons Meeting, in Barcelona, Spain, May of 2009; in part at the British Association of Plastic, Reconstructive, and Aesthetic Surgery Summer Meeting, in Deauville, France, July of 2007; at Research!Louisville, in Louisville, Kentucky, October of 2007; and at the British Burn Association's 40th Annual Scientific Meeting, in Swansea, United Kingdom, April of 2007.

DOI: 10.1097/PRS.0b013e3181c2a5cc

Disclosure: *There are no financial conflicts of interests between any of the authors listed in this article and the work described in it.*

Fig. 1. Quadrilateral full-thickness eyelid loss was reconstructed with mucous membrane and skin grafts. Nearly total tarsorrhaphy is required to prevent corneal desiccation.

and perioral tissues to treat midface and lower facial defects with encouraging preliminary outcomes.[6–8] Replacing damaged or missing periorbital tissues with a healthy periorbital unit allograft is compelling; however, this methodology has yet to be addressed.

In this article, we report our anatomic analysis of myoneural and vascular constituents that are essential to the function of a periorbital and eyelid pair allograft. Specifically, we studied location and constitution of vascular tributaries and facial nerve branches relevant to this unique surgical undertaking. The resulting anatomic knowledge provided the foundation for preservational harvest of a complete periorbital functional unit. To our knowledge, this is the first study to analyze and describe the principal complexities of surgical reconstruction of the periorbital functional unit by allotransplantation of an eyelid pair.

MATERIALS AND METHODS

Twelve fresh cadavers (24 hemifaces, eight male and four female; age range, 49 to 99 years) were dissected and studied using loupe magnification (3.5×) and an operative microscope (OPMI 1F; Zeiss, Oberkochen, Germany; 10 to 25×). A Vernier caliper (1/20 mm; Kanon Instruments, Tokyo, Japan) and a grid (2 mm in 200 parts; E. Leitz GmbH, Wetzlar, Germany) were used to record all measurements. None of the dissected specimens had a history of congenital facial malformation, trauma, or surgery.

Location, pattern, dimensions, and anatomic variations of the surgically relevant external carotid and internal carotid arterial branches and venous tributaries were studied from their proximal origins to the orbicularis oculi. Facial nerve position, diameter, and branch patterns relevant to the orbicularis innervation were measured and mapped.

Based on our anatomic observations and descriptions from the pertinent literature,[6–28] different surgical planes of approach were evaluated. The resulting surgical sequences were designed to preserve essential functional constituents of the periorbital unit, while assuring perfusion and facial nerve input during the entire harvest.

Vascular integrity was evaluated angiographically in seven harvested periorbital units. After the surgical protocol (see Periorbital Unit Harvest Protocol in the Results section), each unit was delicately dissected en-bloc, removed from the cadaver, and fixed to a radiolucent board for imaging. Each of the external carotid arterial branches in five isolated periorbital units was identified, cannulated, injected with radiopaque fluid [Oxilan 350 (Ioxilan), Guerbet Group, Bloomington, Ind.], and flushed with saline. Extravasation of radiopaque fluid was minimized using cauterization (bipolar coagulation) and ligation (monofilament nylon, 9.0 and 10.0). The periorbital allografts were imaged in an angiographic suite (Innova 3100C, GE Healthcare, Waukesha, Wis.). The contribution of each arterial branch to perfusion of the eyelids and the orbital arcades was analyzed by observing radiopaque filling patterns. The venous system was assessed using the same angiographic technique in two isolated periorbital units.

RESULTS

Vascular Anatomy

Proximal superficial temporal and facial vessels demonstrated consistent anatomic location and diameter in all cadavers; however, their distal components demonstrated variability. The frontal branch of the superficial temporal artery was absent in two hemifaces, while that of the superficial temporal vein was missing in five of 18 dissected specimens. The course of the vessels was predominantly linear, although tortuosity was common in the proximal segments of the frontal branch of the superficial temporal artery. The frontal branch of the superficial temporal vein was equally likely to occur superior or inferior to the artery.

The facial vein followed the lateral margin of the artery in all cases. A distinct continuation of the facial to angular vessels, however, was missing in five of 18 hemifaces. In one hemiface, a varicosity was

the only vascular structure identified in the medial canthus. Simultaneous absence of the frontal branch of the superficial temporal artery and facial-to-angular artery continuation was not observed.

Based on observations in six hemifacial specimens, internal carotid branches were found to be unsuitable for primary allograft revascularization due to small caliber (0.6 ± 0.2 mm and 0.8 ± 0.2 mm, respectively) for the supraorbital and supratrochlear arteries. The supraorbital artery bifurcated in four of six hemifaces below the surface of orbicularis oculi. The supratrochlear artery was absent in one hemiface, and tortuosity marked the extraorbital course of both vessels.

Table 1 summarizes the course and diameter of the vessels, and Figure 2 depicts critical anatomic coordinates of the external carotid tributaries.

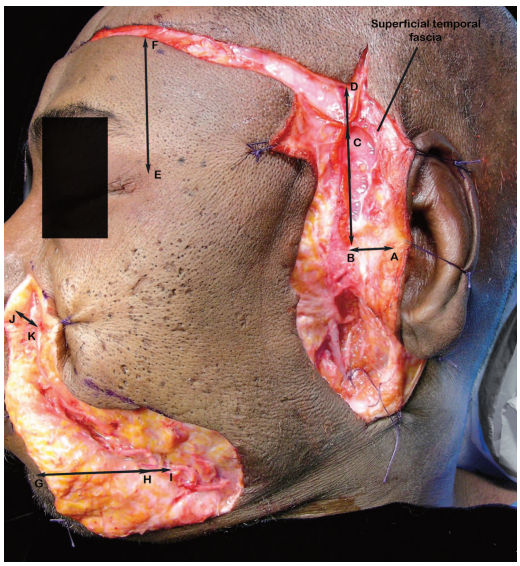

Fig. 2. The topographical coordinates of the external carotid tributaries that supply the periorbital unit depicted here are detailed in Table 1. *AB* denotes distance from the tragus to STA/STV; *BC* and *BD* denote distances to the STA and STV bifurcation, respectively; *EF* denotes distance from the frontal branch of the STA to the lateral canthus; *GH* and *GI* denote distances from the mid–mandibular border to FA/FV at the superior mandibular border; *JK* denotes distance from the nasal ala to FA/FV. *STA*, superficial temporal artery; *STV*, superficial temporal vein; *FA*, facial artery; *FV*, facial vein.

Facial Nerve

Dissection results are presented by facial nerve regions supplying the orbicularis oculi muscle.

Temporal and Superior Zygomatic Nerves

Temporal and superior zygomatic branches bifurcated within the parotid gland, emerging at its superior margin medial to the superficial temporal vessels. Crossing the zygomatic arch, the nerves (and vessels) were intimately apposed to a fascial plane (superficial temporal fascia) that continues cephalad as the galea aponeurotica (Fig. 3).

Temporal branches remained anteroinferior to the frontal branch of the superficial temporal artery (Fig. 3) (see Harvest Protocol, Superficial Temporal Artery Isolation). As the superior zygomatic branches approached the lateral orbicularis oculi margin, they formed a delicate plexiform architecture before entering the posterior muscle surface.

Table 1. Vascular Anatomy: External Carotid Tributaries and Their Correlation to Periorbital Region

No. of Dissected Hemifaces (no. of Dissected Cadavers)	Anatomic Structure	Vascular Cephalometrics			Facial Coordinates*
		Anatomic Location	Diameter (mm)	Surgical Plane	
18 (9)	STA	Anterior to the tragus	–	SMAS	AB = 1.65 ± 0.20 cm
		Proximal to the bifurcation	2.2 ± 0.4	STF	BC = 4.0 ± 0.9 cm
18 (9)	STV	Anterior to the tragus	–	SMAS	Apposition to STA
		Proximal to the bifurcation	2.6 ± 0.5	STF	BD = 4.8 ± 1.2 cm
18 (9)	fSTA	Bifurcation origin	1.8 ± 0.4	STF	BC = 4.0 ± 0.9 cm
		Superior to lateral canthal tendon	–	STF	EF = 4.3 ± 0.6 cm
18 (9)	FA	Superior mandibular border	2.7 ± 0.6	Sub-SMAS	GH = 6.7 ± 0.8 cm
		Lateral to nasal ala	1.2 ± 0.3	Sub-SMAS	JK = 1.5 ± 0.3 cm
18 (9)	FV	Superior mandibular border	3.0 ± 0.8	Sub-SMAS	GI = 7.3 ± 0.9 cm
		Lateral to nasal ala	1.0 ± 0.5	Sub-SMAS	JK = 1.8 ± 0.5 cm

STA, superficial temporal artery; SMAS, superficial musculoaponeurotic system; STV, superficial temporal vein; STF, superficial temporal fascia; fSTA, frontal branch of the superficial temporal artery; FA, facial artery; FV, facial vein.
*Facial coordinates correspond with Figure 2.

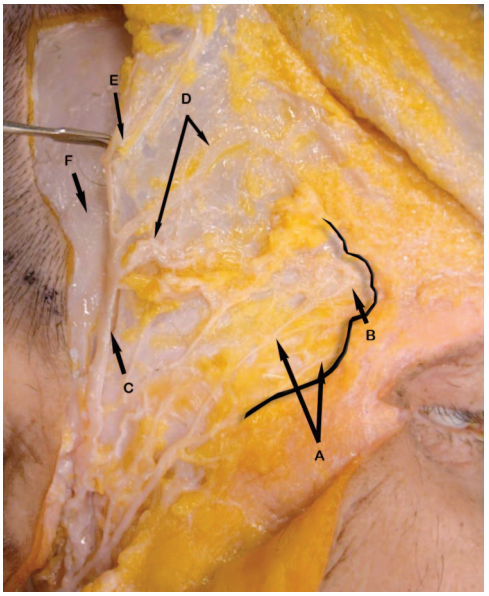

Fig. 3. Discrete distal temporal facial nerve branches (*A*) form plexiform architecture at the margin of the orbicularis oculi muscle (*B*). The superotemporal orbicularis has been removed (the *black line* indicates the medial margin of the resection) to demonstrate the perimuscular facial neural anatomy. Note that the superficial temporal artery (*C*) and its frontal branches (*D*) lie in intimate apposition to the superficial temporal fascia (*E*). Also note the planar distinction between the deep temporal fascia (*F*) and superficial temporal fascia (*E*). Elevating the composite in the plane of the deep temporal fascia (*F*) protects this neurovascular anatomy.

Inferior Zygomatic and Buccal Nerves

Inferior zygomatic branches emerged at the lower medial border of the parotid gland and were in apposition to or fused with the deeper-coursing buccal branch. Both branches passed under the zygomaticus major and minor muscles and levator labii superioris muscle on their medial course. They entered the inferomedial orbicularis oculi, at times in plexiform configuration (Table 2).

Atraumatic skeletonization of intermuscular course of the inferior zygomatic and buccal branches was challenging. Their preservation could be assured only by en-bloc harvest of the zygomaticus major and minor and levator labii muscles (see Harvest Protocol). Table 2 summarizes branch patterns, dimensions, and positional planes of the facial nerve at its origin, medial margin of the parotid gland, and the orbicularis oculi muscle.

Periorbital Unit Harvest Protocol

Harvest of a periorbital unit allograft that retains its functional potential requires (1) preservation of its proximal neurovascular support throughout removal and (2) a release technique that preserves its intricate vascular and myoneural constituents. The surgical sequences described below are designed to maintain composite perfusion during (and after) its removal from the orbital frame.

Superficial Temporal and Facial Artery and Vein Isolation

Superficial Temporal Vessels

Isolation of the distal superficial temporal artery and superficial temporal vein initiates harvest. A cutaneous incision descends to the level of the superficial temporal fascia 1.0 cm medial to the superior pole of the auricle and 4.0 cm cranial to the tragus. Progressive cephalad extension of the skin and fascia incision exposes the vessels to their frontoparietal bifurcations. The arterial branch ascends after bifurcating, then descends to a point approximately 4.3 cm above the lateral canthus (Fig. 2 and Table 1). Thereafter, the vessels join branches of the supraorbital and supratrochlear arteries and veins as they travel to the midline. The cutaneous incision continues to the glabella in the periosteal plane, cephalad to the aforementioned intersections. The proximal superficial temporal artery and superficial temporal vein are subsequently exposed as a prelude to facial nerve isolation (Fig. 4).

Facial Vessels

Facial vessels are located approximately 1.5 cm lateral to the nasal ala (Fig. 2 and Table 1). The artery lies medial to the vein. The distal inferior zygomatic and superior buccal nerve branches to the medial orbicularis lie in the submuscular plane immediately deep to these vessels. After facial vessel isolation, the cutaneous incision turns immediately to the nasal dorsum, at the level of the periosteum. Continuing cephalad, it intersects the transverse frontal incision at midline.

Facial Nerve Isolation

Temporal and Superior Zygomatic Branches

Extending the preauricular incision inferiorly, parallel, and lateral to the course of the superficial temporal vessels provides proximal facial nerve exposure (Fig. 4). Elevation of the superficial musculoaponeurotic system, followed by superficial parotidectomy, reveals temporal and zygomatic nerve bifurcations. As the nerve branches ascend, they are apposed to the superficial temporal fascia (Figs. 3 and 4). Cephalad to the zygomatic arch,

Table 2. Pertinent Extracranial Facial Nerve Anatomy and Its Planar Correlation to the Periorbital Region

No. of Dissected Hemifaces (no. of Dissected Cadavers)	Anatomic Structure (Facial Nerve)	Anatomic Location (Surgical Planes)	No. of Branches*	Diameter (mm)*	Periobital Plexus
14	Main trunk	Lateral and prior to entrance into parotid gland	1	2.6 ± 0.2	
14 (7)	Proximal superior trunk	Inside of the parotid gland	1	1.7 ± 0.4	
14 (7)	Proximal inferior trunk	Inside of the parotid gland	1	1.3 ± 0.4	
14 (7)	Temporal nerve branches	Superior peripheral border of the parotid gland (subparotid-masseteric fascia plane) Superior to zygomatic arch (superficial temporal fascia plane)	1.6 (1–2)	0.8 ± 0.3	
14 (7)	Zygomatic nerve branches	Superomedial border of the parotid gland (subparotid-masseteric fascia plane) At and below zygomatic arch (superficial temporal fascia plane and sub-SMAS plane)	2.5 (2–4)	0.6 ± 0.3	
14 (7)	Buccal nerve branches	Medial border of the parotid gland (subparotid-masseteric fascia plane) Lateral border of superficial facial musculature (sub-SMAS, ventral and dorsal to superficial facial musculature); beware extraplanar branches	3.1 (2–5)	1.0 ± 0.4	
8 (7)	Temporo-zygomatic connection	Lateral to orbicularis oculi muscle (superficial temporal fascia plane)			75%
8 (6)	Zygomatico-buccal connection	Inferior to orbicularis oculi muscle (dorsal to superficial facial musculature)			50%

SMAS, superficial musculoaponeurotic system.
*Number and diameter of facial nerve branches measured at their exit point from the parotid gland.

dissection deep to this layer over the deep temporal fascia releases the superotemporal composite, while protecting nerve branches and vascular tributaries.

Inferior Zygomatic and Buccal Branches

Inferior zygomatic and contiguous superior buccal branches are skeletonized to the lateral border of the zygomaticus major muscle. Thereafter, the nerve branches pass deep to the zygomaticus major, minor, and levator labii muscles before entering the posterior surface of the medial orbicularis. Medial nerve isolation is hampered by its small caliber and serpentine course. Division of the aforementioned muscles inferior to the nerve branch assures preservation. Dissection terminates at the pyriform aperture. (In a clinical harvest, potential coinnervation by inferior zygomatic and buccal branches demands innervation mapping by nerve stimulation to ensure full composite reinnervation potential. This constraint also applies to host débridement.)

Osseous Release of the Periorbital Unit

Medial and Superior Release

After isolation and protection of the proximal neurovascular constituents, final separation of the composite from the orbit begins superomedially. This region harbors critical tributaries to the orbital and eyelid arcades,[9] which are protected by working within the subperiosteal plane. Dissection advances to the medial inferior orbital rim, lysing orbicularis oculi insertions and the medial canthal tendon's osseous attachments. The lacrimal sac is transected at the nasolacrimal duct.

Superomedial dissection resumes at the orbital margin, revealing the trochlea, supraorbital, and supratrochlear vessels as corrugator and orbicularis attachments are released (Fig. 5). Osteotomy of the superior orbital foramen releases the supraorbital nerve, artery, and vein. The supraorbital vein ascends to the eyebrow fat pad. It parallels the orbital rim and interconnects with the superior temporal ve-

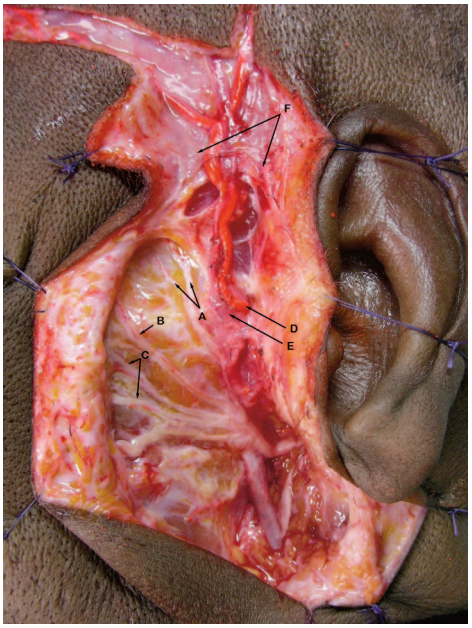

Fig. 4. Proximal facial nerve dissection demonstrates the relationship of the temporal (*A*), zygomatic (*B*), and buccal (*C*) branches to the superficial temporal artery (*D*) and vein (*E*) and the superficial temporal fascia (*F*).

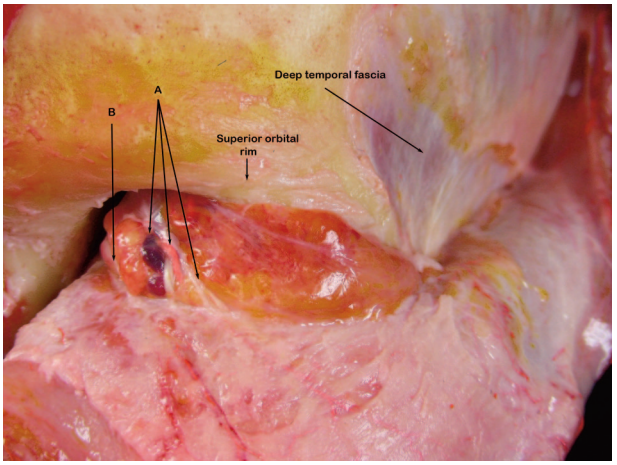

Fig. 5. Supraorbital vessels and nerves (*A*) and supratrochlear artery (*B*) contribute to perfusion of both the supraorbital and eyelid arcades, along with external carotid tributaries. Intraorbital exposure of these internal carotid tributaries preserves anastomotic connections between these two primary eyelid perfusion sources within the eyelid.

nous tributaries, providing venous drainage of the allograft (see also Fig. 10).

Superolateral Release

Subperiosteal elevation tracing the orbital margin to the zygomatic process of the frontal bone and lateral orbital wall completes superolateral release. Separation of the posterior crus of the lateral canthal tendon from the medial zygoma increases tissue mobility, facilitating dissection over the zygomatic arch to the preauricular exposure.

Eyelid Retractor Release and Tarsoconjunctival Harvest

The aforementioned maneuvers allow further composite retraction and lid retractor isolation. Incision of the superior periorbita at the orbital margin exposes the preaponeurotic eyelid adipose tissue. The aponeurosis lies deep to the fat and is followed to the superior tarsal margin. At this coordinate, the peripheral eyelid arcade lies between the aponeurosis and superior sympathetic muscle (Fig. 6).

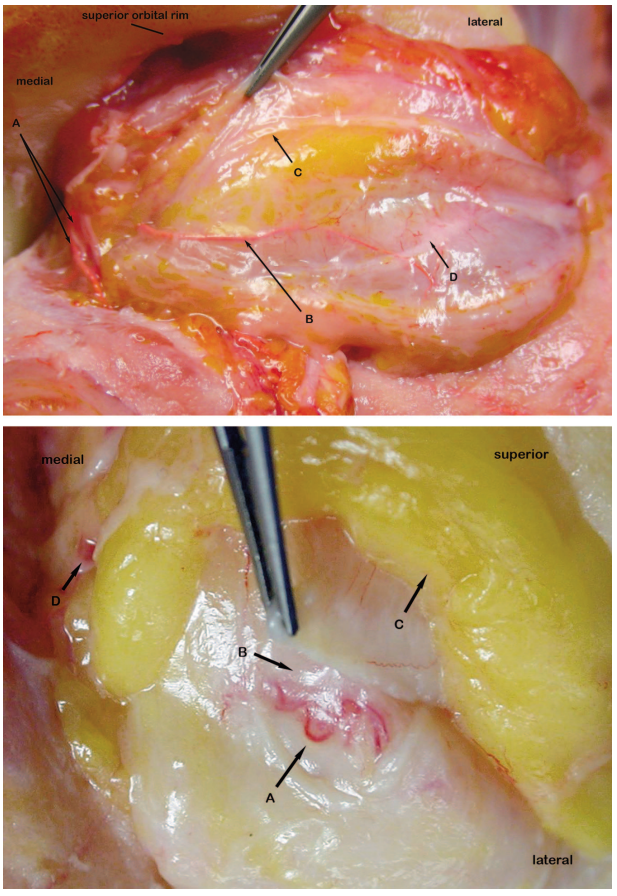

Fig. 6. (*Above*) The medial palpebral artery (*A*) arises from the supratrochlear vessels and descends to the eyelid, supplying the upper and lower eyelid arcades. Division of the distal levator aponeurosis (*C*) reveals the peripheral upper eyelid arcade (*B*), whose origin from the medial palpebral is obscured by medial orbital fat pad. Note the aberrant position of the arcade (*B*) lying on the tarsus (*D*). (*Below*) Forceps hold the cut edge of the distal levator aponeurosis, exposing the peripheral arcade (*A*) lying on Mueller's muscle (*B*). Preaponeurotic fat (*C*) extending from the anterior orbit obscures the levator palpebrae superioris muscle. The medial palpebral artery is concealed by the medial fat pad (*D*).

Through-and-through incision of the retractor-conjunctival composite cephalad to the arcade is first carried to the lateral eyelid. Lacrimal ductules in the superior conjunctival fornix lie superior to the incision plane (assuming preservation of the host lacrimal gland, and its ductules and conjunctiva with accessory tear glands). The distal lacrimal artery is ligated. Medial division of the upper retractors completes superior retractor release. As the incision descends to the lower eyelid and the plica semilunaris, it passes deep to the medial palpebral vessels. The conjunctival incision then resumes caudal to the peripheral arcade, traversing the lower fornix to the lateral eyelid.

Inferior Release

Lower orbicularis attachments to the inferior orbital rim and antral face are separated via the inferior conjunctival incision. Dissection over the maxilla exposes the inferior orbital nerve and vessels, which are ligated and divided.

Terminal Facial Nerve Exposure and Allograft Devascularization

Medial to lateral elevation of the allograft now affords an unobstructed view of the anterior maxilla, the medial margin of the masseter muscle, and the inferior buccal fat pad (ligation of the supraorbital and supratrochlear vessels may be necessary for sufficient composite mobility). Terminal exposure of the proximal facial nerve branches begins in the premasseteric plane, at the inferior margin of the zygomatic arch. Alternating viewing perspective between the premasseteric and lateral dissection planes facilitates nerve branch localization and protects their distal architecture (Figs. 3 and 4). Temporal, zygomatic, and selected buccal branches are tagged and divided near the nerve trunk.

Supratrochlear and supraorbital vessels are ligated within the anterior orbit, preserving anastomotic connections to the orbital and eyelid arcades (i.e., medial palpebral branch of the supratrochlear artery). The superficial temporal vessels are divided at the level of the tragus and the facial vessels at their intersection with the angle of the mandible, completing final release of the periorbital unit form the donor (Fig. 7).

Six periorbital subunits harvested by the foregoing approach required an average operative time of 2.5 ± 0.5 hours by two experienced surgeons (D.V. and M.D.G.) (Fig. 8). In a clinical harvest, modifications to the foregoing technique embrace host injury characteristics, host and donor dynamic vascular features, and host-donor cephalomorphic dimensions.

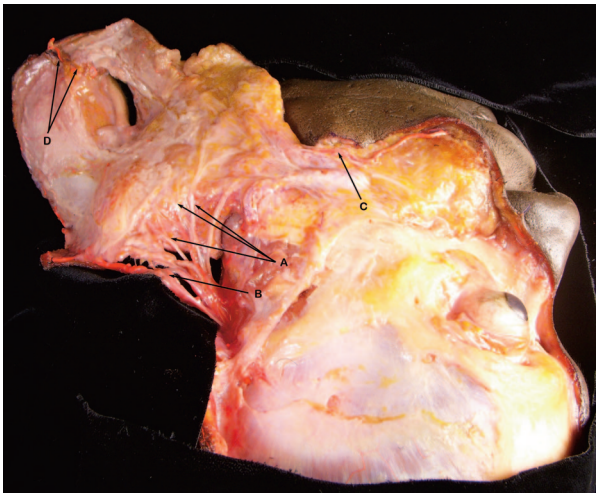

Fig. 7. The final periorbital allograft, before release from the donor, is based on the peripheral branches of the facial nerve and the superficial temporal and facial vessels. The preauricular and premasseteric biplanar dissection planes protect proximal facial nerve branches (*A*) and their terminal arborization at the orbicularis oculi. The vascular supply of the periorbital unit [superficial temporal (*B*) and facial (*C*) vessels] is preserved throughout the dissection by this technique. Note the ligated supraorbital/supratrochlear vessels and medial palpebral artery (*D*).

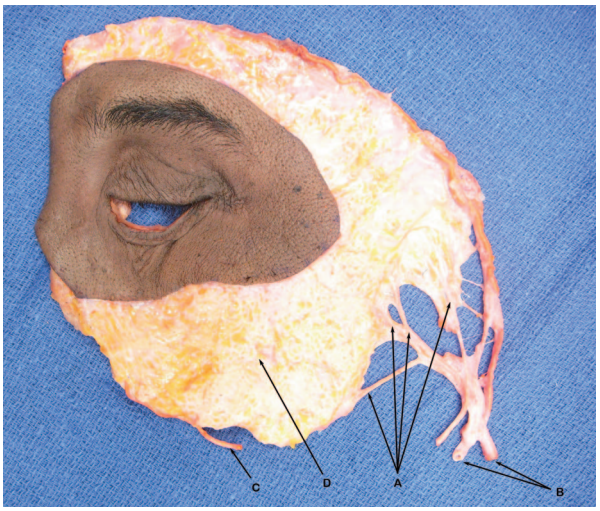

Fig. 8. A harvested periorbital unit demonstrating preserved facial nerve branches (*A*) and the course of superficial temporal (*B*) and facial (*C*) vessels. Also note the retained zygomatic musculature (*D*), which contains the superior buccal branch that innervates the medial orbicularis oculi muscle.

Angiographic Assessment of Allograft Vascular Integrity

Angiographic analysis of the eyelid perfusion patterns was performed in seven harvested periorbital units. Perfusion of the superficial temporal

artery filled both eyelid and orbital arcades in four of five units (Fig. 9). Facial artery injection filled the orbital and eyelid arcades in three of five units. Single selective facial venograms of two allografts showed intact drainage of the periorbital unit in both cases (Fig. 10). These data establish the validity of the harvest protocol and confirm the anatomic vascular variability of the region.

Periorbital Unit Allograft Implantation

Recipient preparation or débridement precedes or occurs simultaneously with harvest to identify skin and mucous membrane requirements and clarify the status of neurovascular tissues. Recipient facial nerve mapping, in particular of the inferior zygomatic and buccal branches, is imperative to ensure full allograft reinnervation potential and avoid the injury to the branches that may coinnervate contiguous facial muscles. In such cases, end-to-side neural anastomosis is considered[29] as a reinnervation option.

Implantation of the periorbital unit into the recipient site largely recapitulates harvest, in modified order, using standard microsurgical and craniofacial techniques. The initial priority is donor-to-host arterial and venous revascularization, followed by nerve repair, reconstitution of host and donor lacrimal excretory components, can-

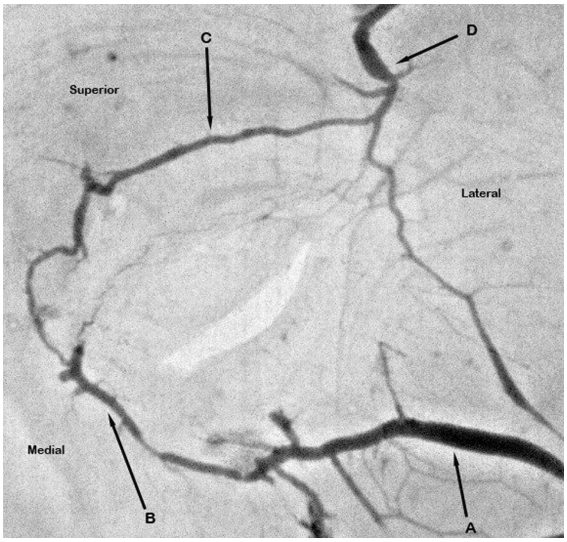

Fig. 10. Facial venous injection demonstrates filling of the facial (*A*), angular (*B*), and superior orbital veins (*C*). Note the potential of the alternative venous drainage route through superficial temporal venous conduits (*D*). Primary venous drainage of the periorbital composite follows venous tributaries that flow terminally to the external jugular vein and via the cavernous sinus. The largest constituent of the network, the superior orbital vein of the internal jugular system, parallels the orbital rim upon exiting the orbit. It joins the superficial temporal venous watershed at the lateral canthus and connects medially with branches of the angular vein.[11]

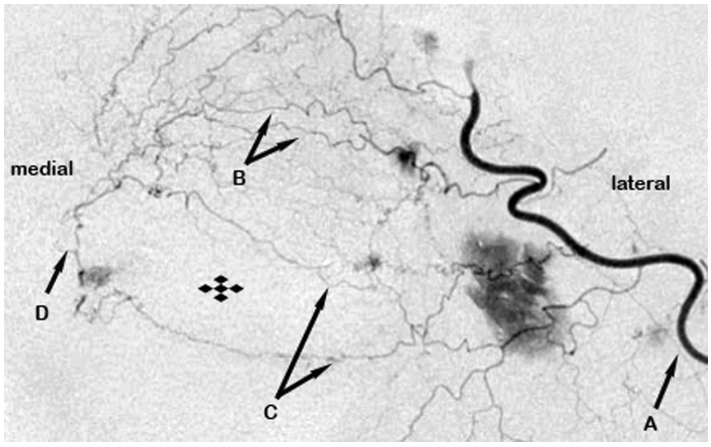

Fig. 9. Superficial temporal arterial injection (*A*) perfuses the orbital (*B*) and eyelid arcades (*C*) via the medial palpebral artery (*D*), indicating preservation of the intrinsic eyelid perfusion system during harvest. The orbital arcades lie on the superficial and deep surfaces of the orbital component of the orbicularis oculi muscle. Anastomotic connections between periorbital branches of the internal and external carotid arteries perfuse the arcades.[9,10,27,28] They connect with the eyelid arcades via tributaries that course over the anterior and posterior orbicular surfaces.[9–11] Accordingly, orbicularis release from the orbit must protect this delicate and vulnerable vascular system. The *diamond* symbol denotes the eyelid aperture.

thal tendon attachment to the orbital margins, attachment of eyelid retractors, and finally, skin closure.

DISCUSSION

Current methods used to reconstruct an eyelid pair must compromise visual function to achieve corneal protection and comfort. The visual handicap is profound and aesthetic results are necessarily unsatisfactory. A composite eyelid pair allotransplant, as described herein, could offer the ultimate reconstructive solution.

Preservation of the eyelid's neurovascular integrity was of utmost importance in harvest design. The myoneural, myocutaneous, and adnexal elements comprising its functional triad were preserved by meticulous adherence to the subperiosteal dissection plane during release of osseous attachments. Biplanar exposure protected the composite's proximal and distal facial nerve branches.

Selective postharvest angiography and venography demonstrated integrity of external carotid vessels, the principal vascular arcades and venous drainage routes within the allografts. Internal carotid tributaries (supraorbital and supratrochlear) demonstrated small caliber and unpredictable course during preliminary dissection and are not primary perfusion sources. Their distal anastomotic connections to the orbital and eyelid arcades, however, are essential to posttransplant perfusion.[9,10]

Several reports document viable facial/scalp replantation based on a single vascular pedicle.[30–34] More recently, perfusion of facial tissue allotransplants[6–8] suggests that effective perfusion of an eyelid composite is probable. The superficial temporal vessels, based on their caliber and extensive interconnections within the composite, are considered the primary revascularization option. In their absence in either donor or recipient, facial vessels provide an alternative.

Our anatomic findings underscore the importance of anatomic variability in reperfusion planning. Absence of the facial-to-angular artery continuation and of the frontal branch of the superficial temporal artery occurred in 28 and 11 percent of hemifaces, respectively. Further, angiographic data showed inconsistent filling pattern of the harvested periorbital units by the superficial temporal artery and facial artery alone. These anatomic results, however, are not equivalent to dynamic perfusion analysis. Accordingly, study of host and donor periorbital arterial and venous phases during selective external carotid angiography is needed to refine reperfusion options.

Although viable wound coverage is the penultimate reconstructive goal, the degree of orbicularis functional recovery is the ultimate measure of allograft effectiveness. Classic end-to-end facial nerve trunk repair restores tonus and volitional blink but rarely reflexive eyelid closure.[35,36] In our model, proximal anastomosis of homologous donor and recipient facial nerve branches preserves the pedicle's distal innervation and that of other recipient facial subunits. Theoretical advantages include direct connection between functionally appropriate nerves, neurorrhaphy in proximity to the target muscle, and single facial muscle denervation. These modifications may improve axon guidance and animation recovery[37–39]; however, absent a comparable model, functional outcomes are unknown.

Facial transplants performed thus far[7] have demonstrated early sensory recovery, but long-term functional outcomes and corresponding reinnervation etiology have yet to be studied.[40] Accordingly, the orbicularis oculi response to the combined stresses of ischemia and denervation, to which its fast-twitch fibers are comparatively vulnerable, is unknown.[41] Of interest, Lantieri et al.[8] in replacing the lower and middle section of the face reported a blink reflex of the autochthonous orbicularis oculi that was absent before surgery.

An eyelid pair allograft may ultimately be included in the reconstructive surgeon's armamentarium. Limitations in estimation of functional potential, however, highlight the need for an animal model to clarify the impact of ischemia, immunological, and denervation effects on posttransplant myoneural reconstitution during allograft recovery.

M. Douglas Gossman, M.D.
2302 Hurstbourne Village Drive, Suite 700
Louisville, Ky. 40299
dgoss@gossmanmd.com

ACKNOWLEDGMENTS

The authors gratefully acknowledge Robert D. Acland, M.D., for his invaluable support, advice, and technical assistance during all stages of this project. They also acknowledge Thomas G. O'Daniel, M.D., and Jacob Yunker, M.D., for their insightful contributions to facial nerve dissections. The authors thank Leigh B. Kleinert and Robert Reed of the Cardiovascular Innovation Institute, Louisville, for their assistance on angiographic data rendition. Cadaver specimens for this study were provided through the Body Bequeathal Program of the University of Louisville School of Medicine. The authors

thank Steve Anderson and Troy Nukes from the program for their help.

REFERENCES

1. Achauer BM, Menick FJ. Salvage of seeing eyes after avulsion of upper and lower lids. *Plast Reconstr Surg.* 1985;75:11.
2. Hay D. Reconstruction of both eyelids following traumatic loss. *Br J Plast Surg.* 1971;24:361.
3. Bedrossian RH, Sperry DW. Repair of avulsion of eyelids and cheek. *Ann Ophthalmol.* 1988;20:31.
4. Thai KN, Billmire DA, Yakuboff KP. Total eyelid reconstruction with free dorsalis pedis flap after deep facial burn. *Plast Reconstr Surg.* 1999;104:1048.
5. Nose K, Isshiki N, Kusumoto K. Reconstruction of both eyelids following electrical burn. *Plast Reconstr Surg.* 1991;88:878.
6. Devauchelle B, Badet L, Lengelé B, et al. First human face allograft: Early report. *Lancet* 2006;368:203.
7. Dubernard J.-M, Lengelé B, Morelon E, et al. Outcomes 18 months after the first human partial face transplantation. *N Engl J Med.* 2007;357:2451.
8. Lantieri L, Meningaud JP, Grimbert P, et al. Repair of the lower and middle parts of the face by composite tissue allotransplantation in a patient with massive plexiform neurofibroma: A 1-year follow-up study. *Lancet* 2008;372:639.
9. Kawai K, Imanishi N, Nakajima H, et al. Arterial anatomical features of the upper palpebra. *Plast Reconstr Surg.* 2004;113: 479.
10. Erdogmus S, Govsa F. Arterial features of inner canthus region: Confirming the safety for the flap design. *J Craniofac Surg.* 2006;17:864.
11. Whitnall SE. *The Anatomy of the Human Orbit.* Huntington, N.Y.: Kreiger Publishing Company Inc.; 1979; pp. 168, 173.
12. Gosain AK, Sewall SR, Yousif NJ. The temporal branch of the facial nerve: How reliably can we predict its path? *Plast Reconstr Surg.* 1997;99:1224.
13. Hwang K, Cho HJ, Chung IH. Pattern of the temporal branch of the facial nerve in the upper orbicularis oculi muscle. *J Craniofac Surg.* 2004;15:373.
14. Hwang K, Jin S, Hwang SH, et al. Innervation of upper orbicularis oris muscle. *J Craniofac Surg.* 2006;17:1116.
15. Nemoto Y, Sekino Y. Anatomical reasons for problems after neurectomy for blepharospasm: A study in cadavers. *Scand J Plast Reconstr Surg Hand Surg.* 2000;34:21.
16. Nemoto Y, Sekino Y, Kaneko H. Facial nerve anatomy in eyelids and periorbit. *Jpn J Ophthalmol.* 2001;45:445.
17. Ouattara D, Vacher C, de Vasconcellos JJA, et al. Anatomical study of the variations in innervation of the orbicularis oculi by the facial nerve. *Surg Radiol Anat.* 2004;26:51.
18. Ramirez OSR. Spatial orientation of motor innervation to the lower orbicularis oculi muscle. *Aesthet Surg J.* 20: 107, 2000.
19. Saylam C, Ucerler H, Orhan M, et al. Anatomic guides to precisely localize the zygomatic branches of the facial nerve. *J Craniofac Surg.* 2006;17:50.
20. Bernstein L, Nelson RH. Surgical anatomy of the extraparotid distribution of the facial nerve. *Arch Otolaryngol.* 1984; 110:177.
21. Davis RA, Anson BJ, Budinger JM, et al. Surgical anatomy of the facial nerve and parotid gland based upon a study of 350 cervicofacial halves. *Surg Gynecol Obstet.* 1956;102:385.
22. Freilinger G, Gruber H, Happak W, et al. Surgical anatomy of the mimic muscle system and the facial nerve: Importance for reconstructive and aesthetic surgery. *Plast Reconstr Surg.* 1987;80:686.
23. Lei T, Xu D-C, Gao J-H, et al. Using the frontal branch of the superficial temporal artery as a landmark for locating the course of the temporal branch of the facial nerve during rhytidectomy: An anatomical study. *Plast Reconstr Surg.* 2005; 116:623.
24. Marano SR, Fischer DW, Gaines C, et al. Anatomical study of the superficial temporal artery. *Neurosurgery* 1985;16:786.
25. Muzaffar AR, Mendelson BC, Adams WP, Jr. Surgical anatomy of the ligamentous attachments of the lower lid and lateral canthus *Plast Reconstr Surg.* 2002;110:873.
26. Rosenstein T, Talebzadeh N, Pogrel MA. Anatomy of the lateral canthal tendon. *Oral Surg Oral Med Oral Pathol Oral Radiol Endod.* 2000;89:24.
27. Sutcliffe T, Baylis HI, Fett D. Bleeding in cosmetic blepharoplasty: An anatomical approach. *Ophthal Plast Reconstr Surg.* 1985;1:107.
28. Tucker SM, Linberg JV. Vascular anatomy of the eyelids. *Ophthalmology* 1994;101:1118.
29. Sundine MJ, Quan EE, Saglam O, et al. The use of end-to-side nerve grafts to reinnervate the paralyzed orbicularis oculi muscle. *Plast Reconstr Surg.* 2003;111:2255.
30. Chen IC, Wan HL. Microsurgical replantation of avulsed scalps. *J Reconstr Microsurg.* 1996;12:105.
31. Gatti JE, LaRossa D. Scalp avulsions and review of successful replantation. *Ann Plast Surg.* 1981;6:127.
32. Thomas A, Obed V, Murarka A, et al. Total face and scalp replantation. *Plast Reconstr Surg.* 1998;102:2085.
33. Wilhelmi BJ, Kang RH, Movassaghi K, et al. First successful replantation of face and scalp with single-artery repair: Model for face and scalp transplantation. *Ann Plast Surg.* 2003;50:535.
34. Nahai F, Hurteau J, Vasconez LO. Replantation of an entire scalp and ear by microvascular anastomoses of only 1 artery and 1 vein. *Br J Plast Surg.* 1978;31:339.
35. House JW, Brackmann DE. Facial nerve grading system. *Otolaryngol Head Neck Surg.* 1985;93:146.
36. Jääskeläinen J, Pyykkö I, Blomstedt G, et al. Functional results of facial nerve suture after removal of acoustic neurinoma: Analysis of 25 cases. *Neurosurgery* 1990;27:408.
37. Brushart TM, Gerber J, Kessens P, et al. Contributions of pathway and neuron to preferential motor reinnervation. *J Neurosci.* 1998;18:8674.
38. Fawcett JW, Keynes RJ. Peripheral nerve regeneration. *Annu Rev Neurosci.* 1990;13:43.
39. Horsch Kw BPR. Functional specificity and somatotopic organization during peripheral nerve regeneration. In Jewett JL, McCarrol HR, eds. *Nerve Repair and Regeneration.* St. Louis, Mo.: Mosby.
40. Guntinas-Lichius O. Outcomes 18 months after the first human partial face transplantation. *N Engl J Med.* 2008;358: 2179.
41. Chan RK, Austen WG, Ibrahim S, et al. Reperfusion injury to skeletal muscle affects primarily type II muscle fibers. *J Surg Res.* 2004;122:54.